Arab J Sci Eng (2014) 39:8121–8133
DOI 10.1007/s13369-014-1356-4

RESEARCH ARTICLE - MECHANICAL ENGINEERING

Buckling Analysis of Functionally Graded Thick Cylindrical Shells with Variable Thickness Using DQM

R. Akbari Alashti · S. A. Ahmadi

Received: 28 September 2013 / Accepted: 31 January 2014 / Published online: 28 August 2014

Abstract In this paper, buckling analysis of a functionally graded thick cylindrical shell with variable thickness subjected to combined external pressure and axial compression is carried out. Moreover, the effect of an axisymmetric imperfection on the buckling load of the shell is investigated. It is assumed that material properties of the shell vary smoothly through the thickness according to a power law distribution of the volume fraction of constituent materials, while the Poisson's ratio is assumed to be constant. The shell is considered to be simply supported at both ends. The governing differential equations are obtained based on the second Piola–Kirchhoff stress tensor and are then reduced to a homogenous linear system of equations using differential quadrature method. Effects of several parameters of the shell including the volume fraction of constituents, geometric ratios, thickness variation amplitude factor, imperfection parameter and loading conditions on the buckling behavior of the functionally graded thick cylindrical shell are investigated. The results obtained by the present method are compared with results reported in the literature.

Keywords Variable thickness · Differential quadrature method · Buckling load · Functionally graded material · Thick cylindrical shell

R. A. Alashti (✉) · S. A. Ahmadi
Mechanical Engineering Department, Babol University of Technology, Shariati Avenue, P.O.Box 484, Babol, Iran
e-mail: raalashti@hotmail.com; raalashti@nit.ac.ir

الخلاصة

تم ـ في هذه الورقة العلمية ـ إجراء تحليل الالتواء من هيكل اسطواني سميك متدرج وظيفيا مع سمك متغير ومتعرض لضغوط خارجية مجتمعة وضغط محوري. وعلاوة على ذلك، فقد تمت دراسة تأثير وجود نقص متناسق مع المحور فيحمل التواء الهيكل. وتم الافتراض أن خصائص مواد الهيكل تتغير بشكل سلس من خلال السماكة وفقا لتوزيع قانون السلطة من جزء حجم المواد المكونة، في حين أفترضت نسبة بواسون لتكون ثابتة. وتم النظر في الهيكل على أنه ببساطة مدعم عند كلا الطرفين. وتم الحصول على المعادلات التفاضلية الحاكمة اعتمادا على موتر إجهاد كيرشوف ـ بيولا الثاني، ومن ثم تم تخفيضها إلى نظام الخطية المتجانسة من المعادلات التفاضلية باستخدام طريقة التربيع. وقد تم التحقيق في آثار العديد من معلمات الهيكل بما في ذلك الجزء من حجم المكونات ، والنسب الهندسية ، وعامل سعة اختلاف السماكة ، ومعلمة النقص وظروف الحمل في سلوك الالتواء لهيكل أسطواني سميك متدرج وظيفيا. وتمت مقارنة النتائج التي تم الحصول عليها من الأسلوب الحالي بالنتائج المعلنة في الأدب.

List of symbols

R_1, R_2	Shell inner, outer radius, respectively
L	Length of the shell
$a(x)$	Mid-surface radius of the shell
$h(x)$	Thickness of the shell
r, θ, x	Radial, circumferential, longitudinal coordinate, respectively
z	Radial coordinate at the mid-surface
h_0	Thickness of a perfect cylindrical shell
η	Thickness variation amplitude
ε	Non-dimensional parameter of the imperfection
α, β	Constant coefficients
k	Volume fraction index
E_m, E_c	Elastic modulus of metal, ceramic, respectively
V_m, V_c	Volume fraction of the metal, ceramic, respectively
$\vec{t}$	Traction vector
$\bar{F}$	Deformation gradient
$\vec{V}$	Displacement vector

I	Unit tensor
F	Axial compressive load
P	Uniform lateral pressure
$\sigma_{ij}, \varepsilon_{ij}$	Stress, strain tensor components, respectively
w, v, u	Displacement fields in r, θ, x directions, respectively
m	Buckling mode number in the circumferential direction
G, λ	Lame coefficients
N	Number of grid points in the r direction
Q	Number of grid points in the x direction
$w_{ij}^{(n)}$	Weighting coefficients of the nth order derivative
$a_{ij}^{(n)}, b_{ij}^{(n)}$	Weighting coefficients of the nth order derivative in the r, x-direction, respectively
P_{cr}	Critical buckling pressure
λ	Ratio of the buckling pressure of the imperfect to the perfect shell
λ'	Ratio of the buckling axial stress of the imperfect to the perfect shell
K	Structural stiffness matrix
ϕ_i	Eigenvector
λ_i	Eigenvalue
S	Stress stiffness matrix

1 Introduction

Cylindrical shells are common structural components in various types of engineering structures. A new class of materials known as functionally graded materials (FGMs) with properties varying continuously along one or more directions have also been introduced that attracted the attention of many researchers. Since these structures are usually under the action of non-uniform loadings such as non-uniform pressure loading, these are required to be made with non-uniform thickness in the axial direction. Comparison of results reported in the literature reveals a large deviation between the theoretical buckling loads of cylindrical shells and experimental ones. One of the main reasons for such discrepancy may be the inevitable differences in the shell geometric characteristics caused by imperfections that are usually produced in manufacturing process or developed in corrosive environments. Buckling analysis of thin cylindrical shells considering geometrical imperfections had been investigated by few researchers.

Koiter [1] and Elishakoff et al. [2] have studied the effect of axisymmetric imperfections with axisymmetric buckling mode shapes on the stability of isotropic and composite cylindrical shells under the action of axial compression loading. Buckling analysis of thin cylindrical shells under the action of lateral pressure considering geometrical imperfection in the circumferential direction was carried out by Gusic et al. [3]. Nguyen and Thach [4] carried out buckling analysis of thin cylindrical panels with variable thickness using the hybrid perturbation-Galerkin method. In another work, they applied the energy method to study the stability of thin imperfect cylindrical panels with thickness variation and initial geometrical imperfections [5]. Buckling behavior of cylindrical shells with axisymmetric imperfection in the axial direction under the action of external pressure was studied by Nguyen et al. [6]. The effect of thickness variation on the buckling load of an isotropic thin cylindrical shell in case of axial compression loading was studied by Elishakoff et al. [7]. Axisymmetric thickness variation and geometric imperfections were assumed. Koiter [8] presented an analytical solution for the buckling load of a perfect, non-uniform cylindrical shell under the axial compression loading. Akbari Alashti and Ahmadi [9] investigated the buckling behavior of isotropic cylindrical shells and curved panels with different boundary conditions under the action of pure external pressure. Koiter et al. [10] has also carried out buckling analysis of an axially compressed cylindrical shell with axisymmetrical variable thickness and initial geometric imperfection. It was found that the buckling load reduction is a linear function of the imperfection parameter when it is small. Sofiyev [11] studied the buckling behavior of an orthotropic composite truncated conical shell with continuously varying thickness subject to a time-dependent external pressure. In his work, stability equations were obtained on the basis of Donnell theory and solved by Ritz method. Civalek [12] carried out a parametric study on the free vibration of rotating laminated cylindrical shells using the method of discrete singular convolution. The approach was found to be simple, accurate and efficient with good rate of convergence. For most engineering problems, closed form solution is nearly impossible to obtain, hence an approximate solution is sought by finding the functional values at certain discrete points. The main challenge at this stage is to find the relationship between the derivatives in the partial differential equation and the function values at grid points. Several numerical discretization techniques have been developed during recent years, namely the finite difference, the finite element and the finite volume methods. These methods generally need many grid points in the domain to achieve results with reasonably good accuracy. As compared with these methods, the differential quadrature (DQ) method can obtain very accurate numerical results employing a considerably smaller number of grid points. Mirfakhraei and Redekop [13] used the differential quadrature method to study the buckling behavior of circular cylindrical shells. Civaleka [14] compared the results obtained by differential quadrature (DQ) and harmonic differential quadrature (HQ) methods. It was that the HQ method leads to more accurate results and needs less less grid points than the DQ method.

In this paper, the effect of axisymmetric thickness variation on the buckling load of a thick cylindrical shell made of isotropic and functionally graded material [15] is investigated. Also, the effect of an assumed axisymmetric imperfection on the buckling load of the shell is studied. The shell is assumed to be simply supported at both ends and subjected to a combination of axial compression and lateral pressure loadings. The differential quadrature method is used to obtain the buckling load of the thick cylindrical shell. Numerical results obtained by three-dimensional stability equations were compared with finite element solutions and results reported in the literature. Effects of various parameters including the grading indices of material properties, mechanical loading combinations, shell thickness variation parameter, imperfection amplitude factor and geometric ratios on the buckling load of the shell are studied.

2 Problem Formulation

A thick cylindrical shell with inner radius R_1, outer radius R_2, length L, mid-surface radius $a(x)$, thickness $h(x)$ and coordinate axes (r, θ, x) is considered, as shown in Figs. 1 and 2 where w, v and u are components of displacement function in the radial, circumferential and longitudinal directions, respectively. The coordinate z is defined in the radial direction at mid-surface of the shell that varies from $-h(x)/2$ at the inner surface to $h(x)/2$ at the outer surface. It is assumed that the shell has a meridional thickness in the longitudinal direction, i.e., the x-direction. The imperfection in the shell thickness is assumed to vary trigonometrically in the axial direction. Variation of the thickness and the imperfection of the shell is shown in Fig. 2a, b, respectively.

The thickness of the shell is assumed to vary according to the following formula:

$$h(x) = h_0 \left(1 + \alpha \cdot \left(\frac{x}{L}\right)^{\eta} - \beta \cdot \varepsilon \cdot \cos \frac{\pi}{L}\left(x - \frac{L}{2}\right)\right) \quad (1)$$

where h_0 is the thickness of a perfect cylindrical shell, η is the thickness variation amplitude factor, ε is the non-dimensional parameter of the imperfection and α and β are constants that take values of 1 and zero as required. The first, second and third terms of above formulation represent the thickness, thickness variation and geometrical imperfection of the shell, respectively. As shown in Fig. 2b, the mid-surface radius $a(x)$ varies in the axial direction while the inner radius R_1 is constant. When $\alpha = 0$ and $\beta = 1$, thicknesses of the shell at two ends are the same for all values of ε, i.e., $h(x) = h_0$ at $x = 0, L$ and $h(x) = h_0(1 - \varepsilon)$ at $x = L/2$. The thickness variation for $\varepsilon = 0.2$ is shown in Fig. 3a. However, when $\alpha = 1$ and $\beta = 0$ we have a shell with variable thickness without imperfection, i.e., the thickness varies from h_0 at the top edge to $2h_0$ at the bottom, as shown in Fig. 3b.

In this study, material properties of the shell are assumed to be isotropic, functionally graded and temperature independent. The Young's modulus of the shell is assumed to be obeying the following formula:

$$E(z) = E_c + E_{mc}\,(V_m)^k\,, \quad E_{mc} = E_m - E_c \quad (2)$$

where V_m is the volume fraction of the metal constituent, k denotes the volume fraction index that varies along the thickness of the shell, E_m and E_c denote the elastic modulus of the metal and the ceramic, respectively.

$$V_m = (0.5 + z/k)^k\,, \quad V_c + V_m = 1 \quad (3)$$

According to above formulation, the Young's modulus vary smoothly from the outer surface of the shell, i.e., at

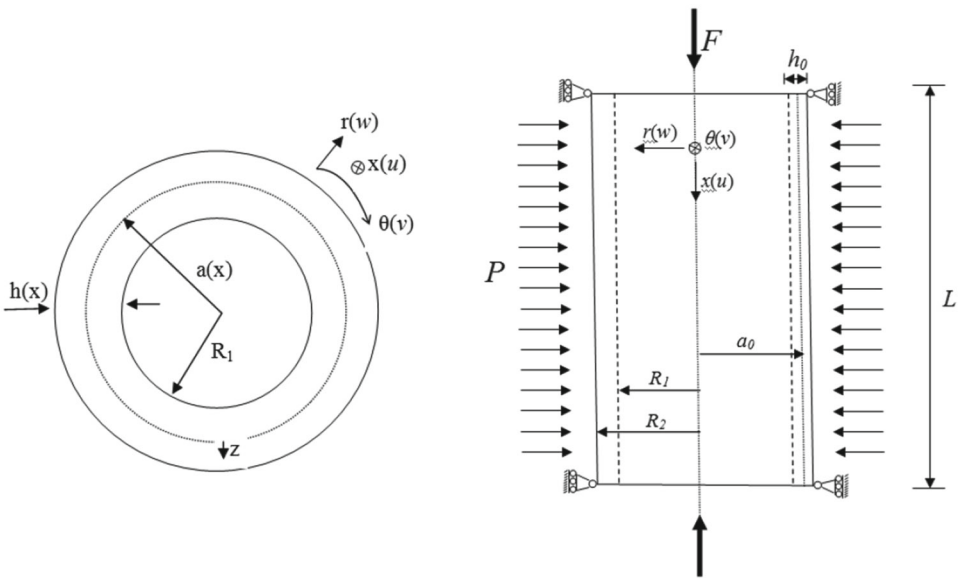

Fig. 1 Cylindrical shell geometry and loading conditions

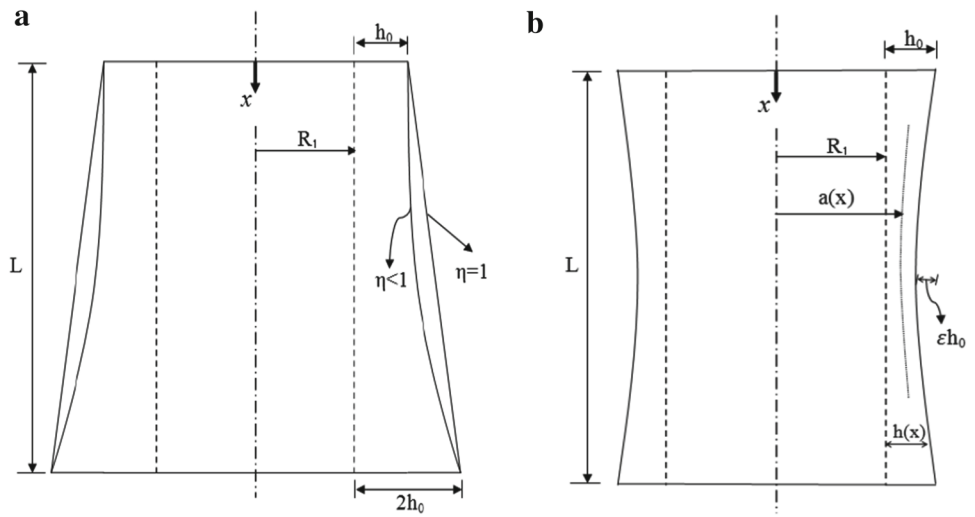

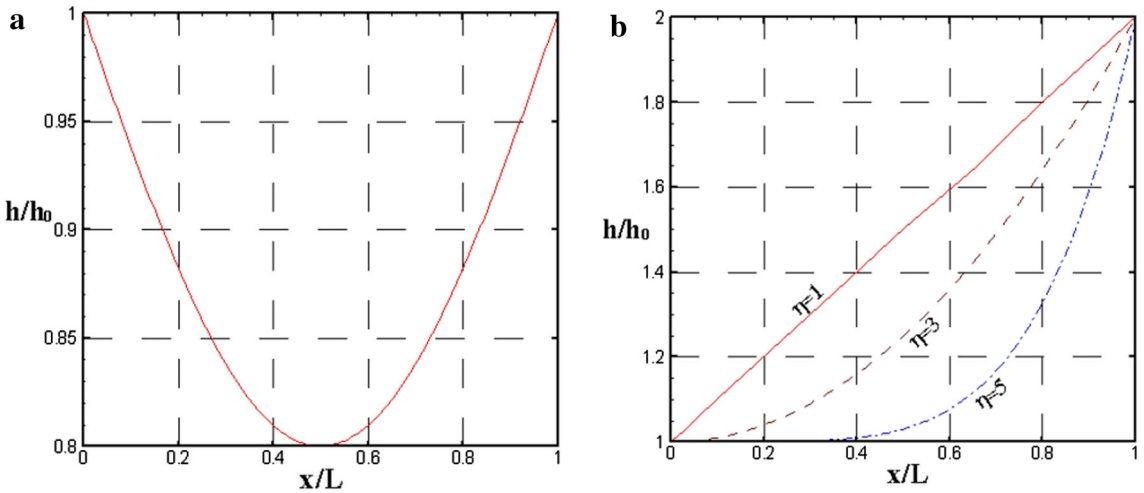

Fig. 2 Thickness variation of the shell. **a** Variable thickness, linear ($\eta = 1$), parabolic ($\eta > 1$). **b** Axisymmetrical imperfection

Fig. 3 Thickness variation form. **a** Imperfection ($\varepsilon = 0.2$). **b** Meridional thickness

$z = h(x)/2$ as a pure metal to the inner surface, i.e., at $z = -h(x)/2$ as a pure ceramic. Boundary conditions of the shell can be written in terms of the second Piola–Kirchhoff tensor σ, using equilibrium equations as:

$$(\bar{F} \cdot \sigma) \cdot \vec{n} = \vec{t}, \quad \bar{F} = I + \text{grad}\vec{V} \tag{4}$$

where $\vec{t}$ is the traction vector, $\vec{n}$ is the outward pointing unit normal vector, $\bar{F}$ is the deformation gradient defined by $\bar{F} = I + \text{grad}\vec{V}$, where $\vec{V}$ is the displacement vector and I is the unit tensor.

Applying Eq. (4) for the outer and inner lateral surfaces in the initial and perturbed equilibrium positions, we can achieve to boundary conditions at lateral surfaces, as follows:

$$\begin{aligned} \sigma'_{rr}\left(a + \frac{h}{2}, \theta\right) &= \sigma'_{rr}\left(a - \frac{h}{2}, \theta\right) = 0 \\ \tau'_{r\theta}\left(a + \frac{h}{2}, \theta\right) &= \tau'_{r\theta}\left(a - \frac{h}{2}, \theta\right) = 0 \end{aligned} \tag{5}$$

$$\tau'_{rx}\left(a + \frac{h}{2}, \theta\right) = \tau'_{rx}\left(a - \frac{h}{2}, \theta\right) = 0$$

In case of thick cylindrical shell, the initial stress components σ^0_{rr} and $\sigma^0_{\theta\theta}$ at the lateral surfaces due to the action of the lateral pressure P, are found to be [16]:

$$\begin{aligned} \sigma^0_{\theta\theta} &= -P\left[1 + \left(\frac{R_1}{r}\right)^2\right] \cdot \left[1 - \left(\frac{R_1}{R_2}\right)^2\right]^{-1} = f_{\theta\theta} \cdot P \\ \sigma^0_{rr} &= -P\left[1 - \left(\frac{R_1}{r}\right)^2\right] \cdot \left[1 - \left(\frac{R_1}{R_2}\right)^2\right]^{-1} = f_{rr} \cdot P \end{aligned} \tag{6}$$

Stress components at two ends of the cylindrical shell under the action of axial compression F are expressed as:

$$\sigma^0_{xx} = -\frac{F}{\pi(R_2^2 - R_1^2)} \tag{7}$$

Assuming a simply supported shell, the following boundary conditions are defined:

$$\text{at } x = 0, L \quad w = v = \sigma'_{xx} = \frac{\partial^2 w}{\partial x^2} = 0 \tag{8}$$

The equilibrium equations are written in terms of the second Piola–Kirchhoff stress tensor σ, in following form [17]:

$$\operatorname{div}(\sigma \cdot \bar{F}^{\mathrm{T}}) = 0 \tag{9}$$

For a three-dimensional problem, Eq. (9) is expanded in the radial, circumferential and axial directions. These equations are presented in simplified forms as follows:

$$\begin{aligned}
&\frac{\partial}{\partial r}\left(\sigma^0_{rr}\varepsilon'_{rr} + \sigma'_{rr}\right) + \frac{1}{r}\frac{\partial}{\partial \theta}(\tau'_{r\theta} + \sigma^0_{\theta\theta}(\varepsilon'_{r\theta} + \omega'_{r\theta})) \\
&\quad + \frac{\partial}{\partial x}\left(\tau'_{rx} + \sigma^0_{xx}(\varepsilon'_{rx} + \omega'_{rx})\right) \\
&\quad + \frac{1}{r}\left(\sigma'_{rr} + \sigma^0_{rr}\varepsilon'_{rr} - \sigma'_{\theta\theta} - \sigma^0_{\theta\theta}\varepsilon'_{\theta\theta}\right) = 0
\end{aligned} \tag{10a}$$

$$\begin{aligned}
&\frac{\partial}{\partial r}\left(\tau'_{r\theta} + \sigma^0_{rr}(\varepsilon'_{r\theta} - \omega'_{r\theta})\right) + \frac{1}{r}\frac{\partial}{\partial \theta}\left(\sigma^0_{\theta\theta}\varepsilon'_{\theta\theta} + \sigma'_{\theta\theta}\right) \\
&\quad + \frac{\partial}{\partial x}\left(\tau'_{\theta x} + \sigma^0_{xx}(\varepsilon'_{\theta x} - \omega'_{\theta x})\right) \\
&\quad + \frac{1}{r}\left(\sigma^0_{rr}(\varepsilon'_{r\theta} - \omega'_{r\theta}) + 2\tau'_{r\theta} + \sigma^0_{\theta\theta}(\varepsilon'_{r\theta} + \omega'_{r\theta})\right) = 0
\end{aligned} \tag{10b}$$

$$\begin{aligned}
&\frac{\partial}{\partial r}\left(\tau'_{rx} + \sigma^0_{rr}(\varepsilon'_{rx} - \omega'_{rx})\right) \\
&\quad + \frac{1}{r}\frac{\partial}{\partial \theta}\left(\sigma^0_{\theta\theta}(\varepsilon'_{\theta x} + \omega'_{\theta x}) + \tau'_{\theta x}\right) \\
&\quad + \frac{\partial}{\partial x}\left(\sigma'_{xx} + \sigma^0_{xx}\varepsilon'_{xx}\right) \\
&\quad + \frac{1}{r}\left(\tau'_{rx} + \sigma^0_{rr}(\varepsilon'_{rx} - \omega'_{rx})\right) = 0
\end{aligned} \tag{10c}$$

In order to calculate buckling loads of thick shells, buckling equations which are developed by authors of the present paper are used [9].

3 Buckling Load Calculation

Considering the boundary conditions stated in Eq. (8), the perturbed displacement field, i.e., u, v and w are found to be in the following forms [9]:

$$\begin{aligned}
w(r,\theta,x) &= B(r,x)\cdot\cos(m\theta) \\
v(r,\theta,x) &= A(r,x)\cdot\sin(m\theta) \\
u(r,\theta,x) &= C(r,x)\cdot\cos(m\theta)
\end{aligned} \tag{11}$$

where m is the buckling mode in the circumferential direction. Substituting Eq. (11) into linear strain–displacement equations and applying the stress–strain relations for isotropic materials, components of the stress field are expressed in terms of components of the displacement field. Substituting the above expression in Eq. (10), the homogenous linear system of equations in the buckled state is obtained:

$$\begin{aligned}
&(2G(z)+\lambda(z))\frac{\mathrm{d}^2B}{\mathrm{d}r^2} + \frac{(2G(z)+\lambda(z))}{r}\frac{\mathrm{d}B}{\mathrm{d}r} \\
&\quad + \frac{m\,(G(z)+\lambda(z))}{r}\frac{\mathrm{d}A}{\mathrm{d}r} + (G(z)+\lambda(z))\frac{\mathrm{d}^2C}{\mathrm{d}r\mathrm{d}x} \\
&\quad - \frac{\left(2G(z)+\lambda(z)+G(z)\cdot m^2\right)}{r^2}B + G(z)\frac{\mathrm{d}^2B}{\mathrm{d}x^2} \\
&\quad - \frac{m\,(3G(z)+\lambda(z))}{r^2}A + \frac{F}{\pi\left(R_2^2-R_1^2\right)}\frac{\mathrm{d}^2B}{\mathrm{d}x^2} \\
&\quad + P\left[\frac{\mathrm{d}}{\mathrm{d}r}\left(f_{rr}\frac{\mathrm{d}B}{\mathrm{d}r}\right) + \frac{f_{rr}}{r}\frac{\mathrm{d}B}{\mathrm{d}r} - \frac{2mf_{\theta\theta}}{r^2}A\right. \\
&\quad \left. - \frac{\left(m^2+1\right)f_{\theta\theta}}{r^2}B\right] = 0
\end{aligned} \tag{12a}$$

$$\begin{aligned}
&G(z)\frac{\mathrm{d}^2A}{\mathrm{d}r^2} + \frac{G(z)}{r}\frac{\mathrm{d}A}{\mathrm{d}r} - \frac{m\,(G(z)+\lambda(z))}{r}\frac{\mathrm{d}B}{\mathrm{d}r} \\
&\quad - \frac{\left(G(z)+m^2\,(2G(z)+\lambda(z))\right)}{r^2}A \\
&\quad + G(z)\frac{\mathrm{d}^2A}{\mathrm{d}x^2} - \frac{m\,(3G(z)+\lambda(z))}{r^2}B \\
&\quad - \frac{m\,(G(z)+\lambda(z))}{r}\frac{\mathrm{d}C}{\mathrm{d}x} + \frac{F}{\pi\left(R_2^2-R_1^2\right)}\frac{\mathrm{d}^2A}{\mathrm{d}x^2} \\
&\quad + P\left[\frac{\mathrm{d}}{\mathrm{d}r}\left(f_{rr}\frac{\mathrm{d}A}{\mathrm{d}r}\right) + \frac{f_{rr}}{r}\frac{\mathrm{d}A}{\mathrm{d}r} - \frac{2mf_{\theta\theta}}{r^2}B\right. \\
&\quad \left. - \frac{\left(m^2+1\right)f_{\theta\theta}}{r^2}A\right] = 0
\end{aligned} \tag{12b}$$

$$\begin{aligned}
&G(z)\frac{\mathrm{d}^2C}{\mathrm{d}r^2} + \frac{G(z)}{r}\frac{\mathrm{d}C}{\mathrm{d}r} + (G(z)+\lambda(z))\frac{\mathrm{d}^2B}{\mathrm{d}r\mathrm{d}x} - \frac{Gm^2}{r^2}C \\
&\quad + (2G(z)+\lambda(z))\frac{\mathrm{d}^2C}{\mathrm{d}x^2} \\
&\quad + \frac{m\,(G(z)+\lambda(z))}{r}\frac{\mathrm{d}A}{\mathrm{d}x} + \frac{(G(z)+\lambda(z))}{r}\frac{\mathrm{d}B}{\mathrm{d}x} \\
&\quad + \frac{F}{\pi\left(R_2^2-R_1^2\right)}\frac{\mathrm{d}^2C}{\mathrm{d}x^2} \\
&\quad + P\left[\frac{\mathrm{d}}{\mathrm{d}r}\left(f_{rr}\frac{\mathrm{d}C}{\mathrm{d}r}\right) + f_{rr}\frac{\mathrm{d}^2C}{\mathrm{d}r} - \frac{m^2f_{\theta\theta}}{r^2}C\right. \\
&\quad \left. + \frac{f_{rr}}{r}\frac{\mathrm{d}C}{\mathrm{d}r}\right] = 0
\end{aligned} \tag{12c}$$

At the next stage, the differential quadrature method is employed to discretize the governing differential equations using the approximation of derivatives of the function $f(x)$ by linear sums of all functional values in the domain:

$$\frac{\mathrm{d}^n f}{\mathrm{d}x}\Big|_{x=x_i} = \sum_{j=1}^{N} w_{ij}^{(n)}\cdot f(x_j) \quad \text{for } i = 1,2,\ldots,N \tag{13}$$

where $w_{ij}^{(n)}$ are the weighting coefficients of the nth order derivative and N denotes the number of grid points in the domain. It should be noted that different values of weighting coefficients are obtained for different grid points, x_i. The most common methods to determine the weighting coefficients are polynomial and Fourier expansion methods. In this study, the polynomial expansion based differential quadrature is used to approximate the first and the second order derivations both in the radial and the longitudinal directions. The weighting coefficients of the first order derivatives are defined as [18].

$$w_{ij}^{(1)} = \frac{M^{(1)}(x_i)}{(x_i - x_j)\cdot M^{(1)}(x_j)} \quad \text{for } i \neq j;$$
$$w_{ii}^{(1)} = \frac{M^{(2)}(x_i)}{2M^{(1)}(x_j)} \tag{14}$$

where

$$M^{(1)}(x_i) = \prod_{k=1,k\neq i,j}^{N} (x_i - x_k),$$
$$M^{(2)}(x) = N^{(2)}(x, x_k)\cdot(x - x_k) + 2\cdots N^{(1)}(x, x_k),$$
$$N(x, x_k) = M^{(1)}(x_i)\cdot\delta_{ij} \tag{15}$$

and for higher order derivatives:

$$w_{ij}^{(n)} = n\left(w_{ij}^{(1)} w_{ii}^{(n-1)} - \frac{w_{ij}^{(n-1)}}{x_i - x_j}\right),$$
$$\text{for } i, j = 1, 2, \ldots, N;\ n = 2, 3, \ldots, N-1;$$
$$w_{ii}^{(n)} = -\sum_{j=1,j\neq i}^{N} w_{ij}^{(n)} \tag{16}$$

Now, using unequal spacing scheme for sampling points in the domain and applying above formulation to Eq. (12), we have:

$$(2G(z)+\lambda(z))\sum_{k=1}^{N} a_{ik}^{(2)} B_{kj} + \frac{(2G(z)+\lambda(z))}{r}\sum_{k=1}^{N} a_{ik}^{(1)} B_{kj}$$
$$+G(z)\sum_{k=1}^{Q} b_{jk}^{(2)} B_{ik} + (G(z)+\lambda(z))\sum_{k=1}^{N}\sum_{l=1}^{Q} a_{ik}^{(1)} b_{jl}^{(1)} B_{kl}$$
$$-\frac{\left(2G(z)+\lambda(z)+G(z)\cdot m^2\right)}{r^2} B_{ij}$$
$$+\frac{m\,(G(z)+\lambda(z))}{r}\sum_{k=1}^{N} a_{ik}^{(1)} A_{kj} - \frac{m\,(3G(z)+\lambda(z))}{r^2} A_{ij}$$
$$+\frac{F}{\pi\left(R_2^2 - R_1^2\right)}\sum_{k=1}^{Q} b_{jk}^{(2)} B_{ik}$$
$$+P\left[\frac{\mathrm{d}f_{rr}}{\mathrm{d}r}\sum_{k=1}^{N} a_{ik}^{(1)} B_{kj} + f_{rr}\sum_{k=1}^{N} a_{ik}^{(2)} B_{kj}\right.$$
$$\left.+\frac{f_{rr}}{r}\sum_{k=1}^{N} a_{ik}^{(1)} B_{kj} - \frac{2mf_{\theta\theta}}{r^2} A_{ij} - \frac{\left(m^2+1\right) f_{\theta\theta}}{r^2} B_{ij}\right] = 0 \tag{17a}$$

$$G(z)\sum_{k=1}^{N} a_{ik}^{(2)} A_{kj} + \frac{G(z)}{r}\sum_{k=1}^{N} a_{ik}^{(1)} A_{kj}$$
$$-\frac{m\,(G(z)+\lambda(z))}{r}\sum_{k=1}^{N} a_{ik}^{(1)} B_{kj}$$
$$-\frac{m\,(3G(z)+\lambda(z))}{r^2} B_{ij} + G(z)\sum_{k=1}^{Q} b_{jk}^{(2)} A_{ik}$$
$$-\frac{\left(G(z)+m^2\,(2G(z)+\lambda(z))\right)}{r^2} A_{ij}$$
$$-\frac{m\,(G(z)+\lambda(z))}{r}\sum_{k=1}^{Q} b_{jk}^{(1)} C_{ik}$$
$$+\frac{F}{\pi\left(R_2^2 - R_1^2\right)}\sum_{k=1}^{Q} b_{jk}^{(2)} A_{ik}$$
$$+P\left[\frac{\mathrm{d}f_{rr}}{\mathrm{d}r}\sum_{k=1}^{N} a_{ik}^{(1)} A_{kj} + f_{rr}\sum_{k=1}^{N} a_{ik}^{(2)} A_{kj}\right.$$
$$\left.+\frac{f_{rr}}{r}\sum_{k=1}^{N} a_{ik}^{(1)} A_{kj} - \frac{2mf_{\theta\theta}}{r^2} B_{ij} - \frac{\left(m^2+1\right) f_{\theta\theta}}{r^2} A_{ij}\right] = 0 \tag{17b}$$

$$G(z)\sum_{k=1}^{N} a_{ik}^{(2)} C_{kj} + \frac{G(z)}{r}\sum_{k=1}^{N} a_{ik}^{(1)} C_{kj}$$
$$+(G(z)+\lambda(z))\sum_{k=1}^{N}\sum_{l=1}^{Q} a_{ik}^{(1)} b_{jl}^{(1)} B_{kl}$$
$$+(2G(z)+\lambda(z))\sum_{k=1}^{Q} b_{jk}^{(2)} A_{ik} - \frac{Gm^2}{r^2} C_{ij}$$
$$+\frac{m\,(G(z)+\lambda(z))}{r}\sum_{k=1}^{Q} b_{jk}^{(1)} A_{ik}$$
$$+\frac{(G(z)+\lambda(z))}{r}\sum_{k=1}^{Q} b_{jk}^{(1)} B_{ik} + \frac{F}{\pi\left(R_2^2 - R_1^2\right)}\sum_{k=1}^{Q} b_{jk}^{(2)} C_{ik}$$
$$+P\left[\frac{\mathrm{d}f_{rr}}{\mathrm{d}r}\sum_{k=1}^{N} a_{ik}^{(1)} C_{kj} + f_{rr}\sum_{k=1}^{N} a_{ik}^{(2)} C_{kj}\right.$$
$$\left.+f_{rr}\sum_{k=1}^{N} a_{ik}^{(2)} C_{kj} - \frac{m^2 f_{\theta\theta}}{r^2} C_{ij} + \frac{f_{rr}}{r}\sum_{k=1}^{N} a_{ik}^{(1)} C_{kj}\right] = 0 \tag{17c}$$

where $a_{ij}^{(n)}$ and $b_{ij}^{(n)}$ denote weighting coefficients of the nth order derivative in the r- and x-direction, respectively. N and Q are number of grid points in the r- and x-direction,

respectively. The critical value of the external pressure, i.e., the buckling load is obtained by solving the set of equations presented in the matrix form as:

$$\begin{bmatrix} [BB] & [BD] \\ [DB] & [DD] \end{bmatrix} \begin{bmatrix} d_b \\ \begin{bmatrix} u \\ v \\ w \end{bmatrix} \end{bmatrix} = P \begin{bmatrix} 0 & 0 \\ [DBG] & [DDG] \end{bmatrix} \quad (18)$$

where sub-matrices $[BB]$, $[BD]$ and $[DBG]$, $[DD]$, $[DB]$, $[DDG]$ are calculated from the boundary conditions and governing equations, respectively. Equation (18) is transformed into the standard eigenvalue problem of the following form:

$$(-[DBG][BB]^{-1}[BD]+[DDG])^{-1}(-[DB][BB]^{-1}[BD]+[DD])$$
$$\begin{bmatrix} u & v & w \end{bmatrix}^{\mathrm{T}} - P[\mathrm{I}]\begin{bmatrix} u & v & w \end{bmatrix}^{\mathrm{T}} = 0 \quad (19)$$

From which, the eigenvalues of P can be found. The smallest value of P is found to be the buckling pressure P_{cr}. For the compressive loading case, the axial load is assumed to be a fraction of the lateral pressure, i.e., $\sigma_x = q \cdot P$, where q is the axial load factor.

4 Numerical Results and Discussion

Accuracy of results obtained by the present method were compared with those of an isotropic homogeneous thick cylindrical shell without imperfection and thickness variation, i.e., $\alpha = 0$ and $\beta = 0$, as reported in [19–21] which were found to be in good agreement [9].

In order to validate the results for an imperfect thick shell, the finite element bifurcation buckling analysis of the thick cylindrical shell is carried out using ANSYS suite of program. The basic form of the eigen-buckling analysis is:

$$[K]\{\phi_i\} = \lambda_i [S]\{\phi_i\} \quad (20)$$

where K, ϕ_i, λ_i and S are the structural stiffness matrix, eigenvector, eigenvalues and stress stiffness matrix, respectively. An eight-noded quadrilateral shell element, namely Shell281, is used to model the thick cylindrical shell. The element can handle membrane, bending and transverse shear effects and is able to form the curvilinear surface satisfactorily.

To study the buckling behavior of a constant thickness shell with imperfection, i.e., $\alpha = 0$ and $\beta = 1$, quantities namely, λ and λ' denoting ratios of the buckling loads of the imperfect shell to the perfect shell are defined:

$$\lambda = \frac{P_{\mathrm{cr}}^{(\mathrm{imper})}}{P_{\mathrm{cr}}^{(\mathrm{per})}}, \quad \lambda' = \frac{\sigma_{\mathrm{cr}}^{x(\mathrm{imper})}}{\sigma_{\mathrm{cr}}^{x(\mathrm{per})}} \quad (21)$$

The buckling load reduction parameter λ for pure external pressure loading cases of an isotropic homogeneous thick shell with imperfection and without thickness variation, i.e., $\alpha = 0$ and $\beta = 1$ are shown in Fig. 4a, b which proposes the same pattern as presented by Nguyen et al. [6]. The ratio of λ' for imperfect thick cylindrical shells made of aluminum under the action of axial loading obtained by the present method, are compared with finite element results as presented in Table 1 which indicates a very good agreement between results obtained by these methods when the imperfection parameter ε, is small.

Variation of buckling loads, i.e., uniform external pressure, axial compression and combined loading with the imperfection parameter ε, for various ratios of the external to internal radius of the shell with $L/a_0 = 1$, are shown in

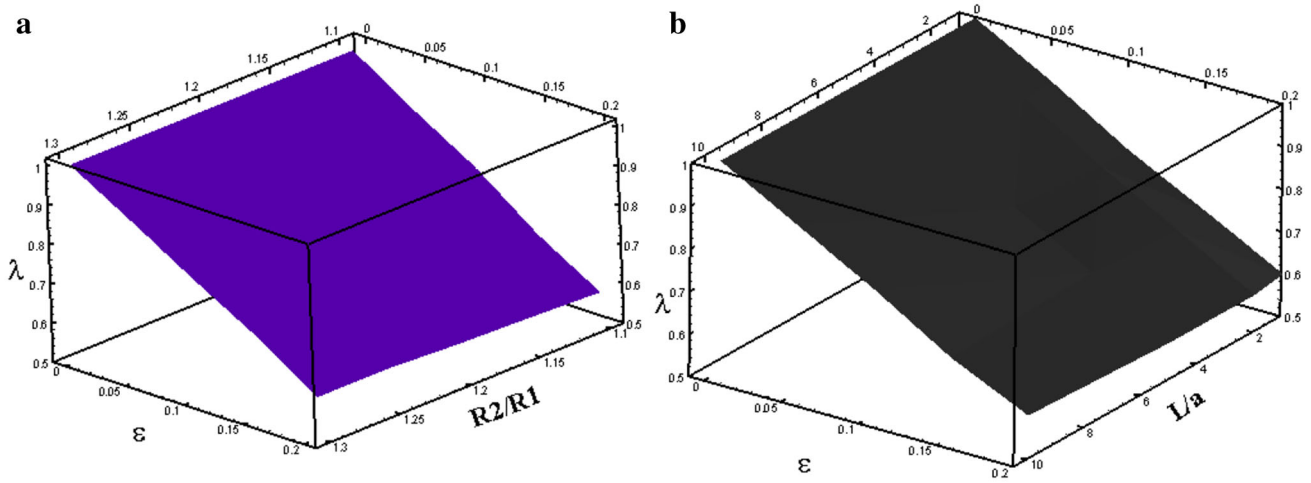

Fig. 4 Variation of buckling load reduction λ with ε and geometric ratios for an isotropic homogeneous shell ($\alpha = 0, \beta = 1$), $m = 2.7\sqrt{a_0/L}\sqrt[4]{a_0/h_0}$

Table 1 Critical stress for pure axial loading of an isotropic homogenous shell $E = 70$ GPa, $R_1 = 1$ m, $R_2 = 1.25$ m, $\nu = 0.3$, $L/a_0 = 1, m = 4$

ε	Present paper		FEM		Difference (%)
	σ_{cr}^{x}(Gpa)	λ'	σ_{cr}^{x}(Gpa)	λ'	
0	14.50	1	13.9	1	4.16
0.01	14.45	0.997	13.817	0.994	4.38
0.05	14.16	0.977	13.483	0.970	4.78
0.10	14.00	0.966	13.401	0.964	4.28
0.15	13.45	0.928	12.927	0.930	3.89
0.20	13.10	0.903	12.635	0.909	3.55

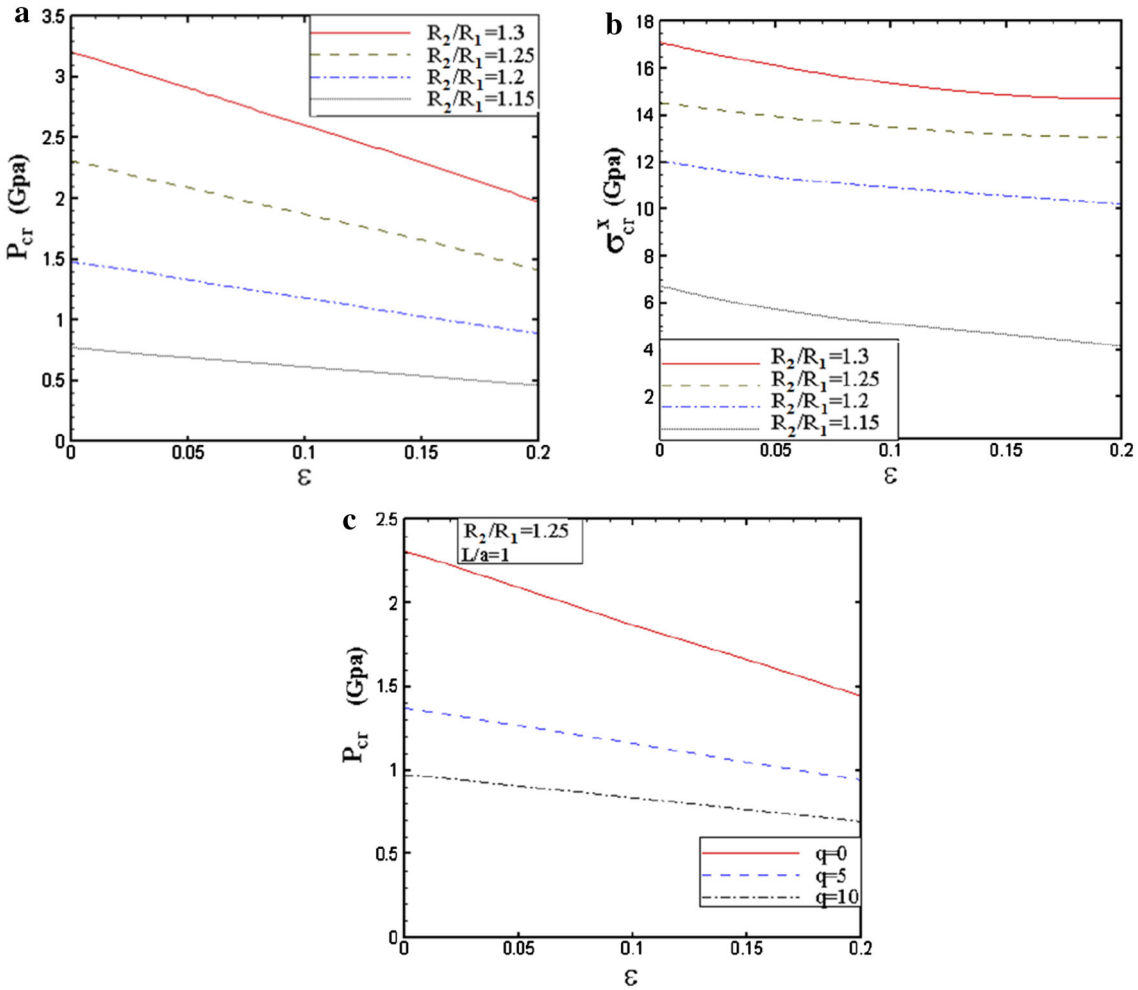

Fig. 5 Variation of critical load with ε, isotropic homogeneous shell ($\alpha = 0$, $\beta = 1$), $E = 70$ Gpa, $m = 2.7\sqrt{a_0/L}\sqrt[4]{a_0/h_0}$. **a** External pressure. **b** Axial compression. **c** Combined loading

Fig. 5a–c, respectively. As noted above, for the combined loading case, the axial load is defined as a fraction of the lateral pressure, i.e., $\sigma_x = q.P$. It can be observed from Fig. 5a, b that for small values of ε and in the case of pure lateral pressure loading, buckling loads are more sensitive to the imperfection amplitude factor ε. In other words, in the case of axial loading, reduction of buckling loads versus ε is smaller than the case of lateral pressure loading. It is also observed from Fig. 5c that the rate of reduction of the buckling load decreases as the load factor increases.

Next, the effect of thickness variation on the buckling load of an isotropic homogeneous thick cylindrical shell under various loading conditions is investigated. The shell is assumed to be a perfect shell, i.e., $\beta = 0$ and $L/a_0 = 1$. Buckling loads for different values of thickness variation amplitude factor η are presented in Fig. 6a–c. It is evident

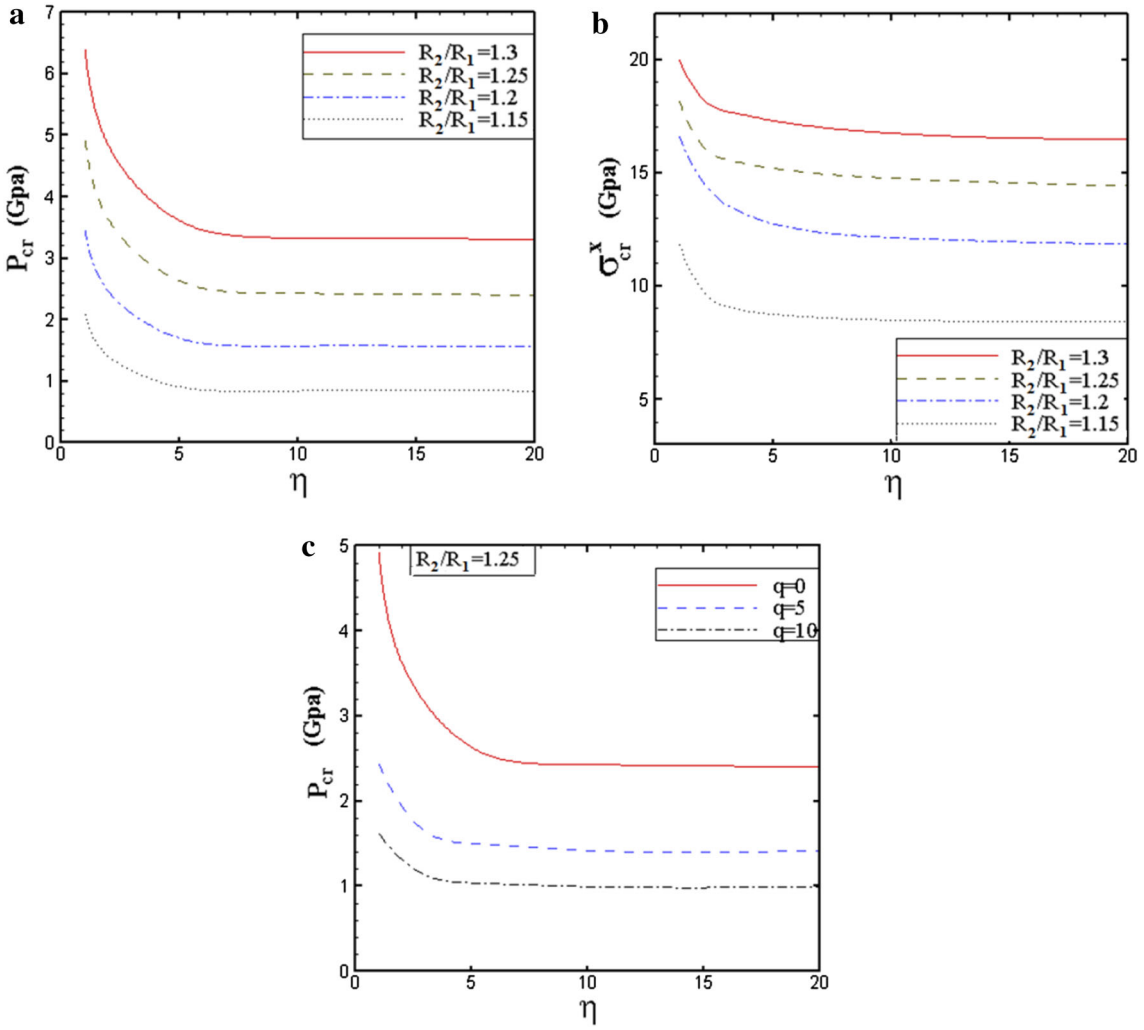

Fig. 6 Critical load versus η for an isotropic homogeneous shell ($\alpha = 1, \beta = 0$), $m = 2.7\sqrt{a_0/L}\sqrt[4]{a_0/h_0}$, $E = 70$ Gpa. **a** External pressure. **b** Axial compression. **c** Combined loading

from Figs. 6a, b that thickness variation has higher effect on the buckling behavior of shell under lateral pressure loading in comparison with the axial loading case. For this type of shell, the buckling load reduces as the parameter η increases and the rate of decrease in case of the lateral pressure loading is found to be higher than the axial compression loading.

Variation of critical loads with mode number of an isotropic homogeneous thick shell with imperfection and thickness variation for the case of pure external pressure loading are presented in Fig. 7a, b, respectively. It is observed from these figures that the critical load for higher values of m approaches an asymptotic value. Variation of critical loads with m, for a thick shell with variable thickness and imperfection, i.e., $\alpha = 1$ and $\beta = 1$ subjected to combined loading is shown in Fig. 7c.

The buckling load results for an isotropic homogeneous shell under the action of pure lateral pressure considering the effect of both imperfection and thickness variation, i.e., $\alpha = 1$ and $\beta = 1$ are shown in Fig. 8. It is shown in the previous section that for a shell with constant thickness, the buckling load ratio reduces linearly for small values of the imperfection factor, ε. As it could be expected, the result presented in Fig. 8 shows that as the thickness parameter η increases and the shell thicknesses approaches a constant value of h_0, the buckling loads ratio λ reduces linearly.

In order to illustrate results of the present method for an inhomogeneous shell, a functionally graded cylindrical shell made of aluminum and alumina is considered. The Young's modulus is assumed to be temperature independent and vary smoothly in the radial direction according to a power law distribution of the volume fraction of the constituent materials. The Young's modulus for the alumina at the inner surface and for the aluminium at the outer surface are assumed to be $E_c = 380$ GPa and $E_m = 70$ GPa, respectively. It is also

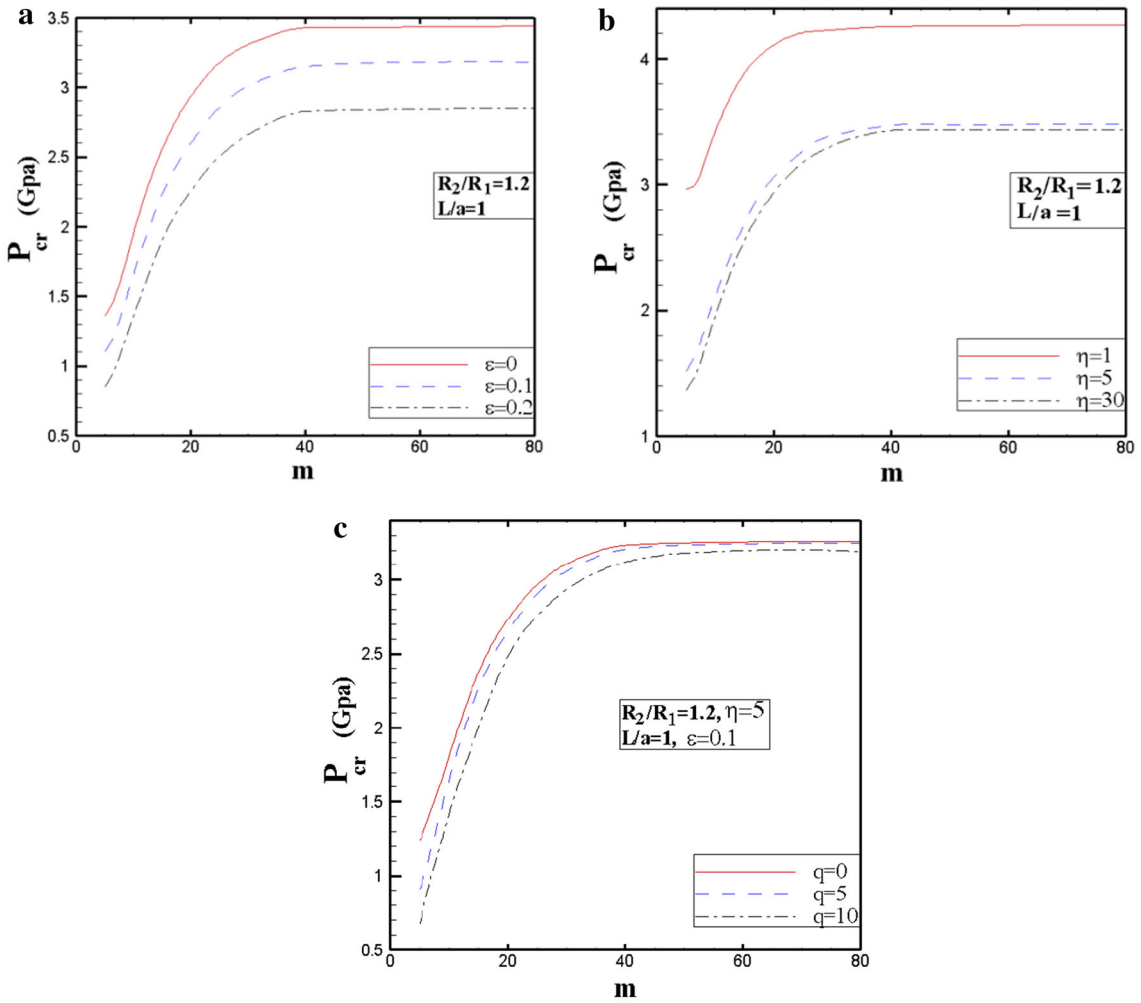

Fig. 7 Critical load versus m for an isotropic homogeneous shell, $E = 70$ Gpa. **a** Imperfection. **b** Variable thickness. **c** Variable thickness with imperfection

assumed that the Poisson's ratios of constituent materials are constant and equal to 0.3. The reduction buckling load ratios, λ and λ' for an imperfect functionally graded thick cylindrical shell with constant thickness, i.e., $\alpha = 0$ and $\beta = 1$ subjected to pure external pressure and axial compression are presented in Table 2. It is shown that as the imperfection parameter ε increases, buckling load for the pure external pressure loading case reduces at higher rate than the pure axial loading case and such reduction for the external pressure loading is linear for small values of ε. The effect of radius ratios on the critical buckling pressure of the uniform thickness shell ($\alpha = 0, \beta = 0$) with $k = 1$ and for mode numbers $m = 6$ and $n = 2$ are presented in Fig. 9.

Critical loads of thick FG cylindrical shells with variable thickness, i.e., $\alpha = 1$ and $\beta = 0$, for different values of k, under the action of lateral pressure and axial compression are illustrated in Fig. 10a, b, respectively. As shown in these figures, critical loads increase as the value of k increases. The main reason for such an increase is the fact that a higher value of k corresponds to a ceramic-rich shell, which usually has higher stiffness than a metal-rich one.

The critical buckling pressures for an isotropic inhomogeneous shell with different values of volume fraction indices are listed in Table 3. It is assumed that the shell is under the action of pure lateral pressure. Effects of both geometrical parameters namely thickness variation and imperfection are studied. According to Eq. (1), as the thickness variation parameter η increases, the thickness approaches a constant value of h_0 for a considerable length of the shell. It is shown in Table 3 that as η increases, the buckling pressure reduces. It is also found that for higher values of η, as the imperfection parameter ε increases buckling load reduction becomes a linear function of the ε for different values of volume fraction index.

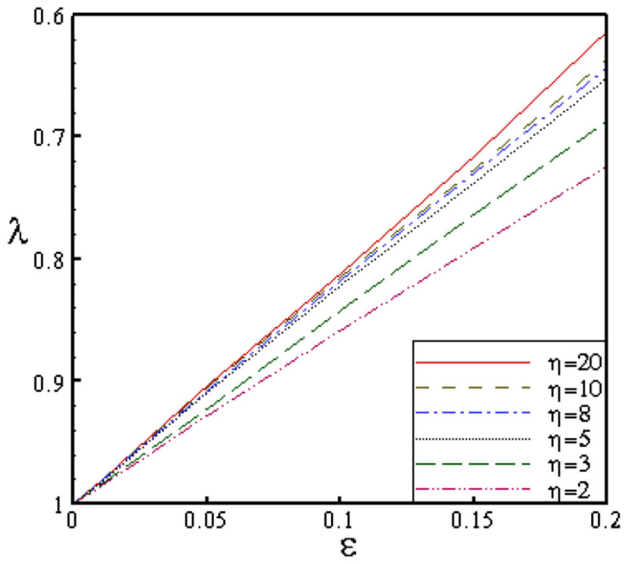

Fig. 8 Variation of buckling load ratio λ of an isotropic homogeneous thick shell with imperfection and thickness variation ($\alpha = 1, \beta = 1$), $R_2/R_1 = 1.25$, $L/a_0 = 1$, $m = 2.7\sqrt{a_0/L}\sqrt[4]{a_0/h_0}$

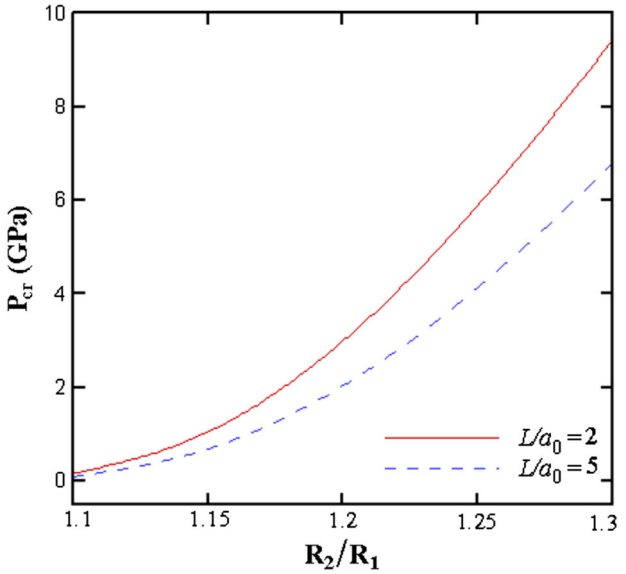

Fig. 9 Variation of buckling pressure of the FG uniform thickness shells ($k = 1$) with radius ratios, $(m, n) = (6, 2)$

Table 2 Critical loads for an FG thick shell versus ε, ($\alpha = 0, \beta = 1$) $R_2/R_1 = 1.25$, $L/a_0 = 1$, $m = 2.7\sqrt{a_0/L}\sqrt[4]{a_0/h_0}$

k	ε	Present paper P_{cr}(Gpa)	λ	Present paper σ^x_{cr}(Gpa)	λ′
0	0	2.307	1	14.50	1
	0.01	2.270	0.984	14.45	0.997
	0.05	2.091	0.906	14.16	0.977
	0.10	1.872	0.811	14.00	0.966
	0.15	1.661	0.719	13.45	0.928
	0.20	1.410	0.611	13.10	0.903
1	0	6.217	1	38.21	1
	0.01	6.10	0.981	38.01	0.995
	0.05	5.62	0.904	37.40	0.979
	0.10	5.05	0.812	37.15	0.973
	0.15	4.42	0.711	36.01	0.942
	0.20	3.80	0.611	34.50	0.903
10	0	11.77	1	73.70	1
	0.01	11.55	0.981	73.31	0.995
	0.05	10.66	0.906	72.50	0.984
	0.10	9.580	0.814	71.44	0.971
	0.15	8.425	0.715	69.40	0.942
	0.20	7.23	0.614	66.4	0.901

The effects of the ratio of the length to the mid-plane radius, i.e., L/a_0 on the critical load of an FG cylindrical shell, subjected to uniform lateral pressure for two separate cases of a shell with variable thickness and with imperfections are shown in Fig. 11a, b, respectively. As it is realized from Fig. 11, as the ratio of L/a_0 increases, the buckling loads approaches an asymptotic value.

Table 3 Critical pressure (GPa) for an FG thick shell versus η and ε, ($\alpha = 1, \beta = 1$), $R_2/R_1 = 1.2$, $L/a_0 = 1$, $m = 4$

ε	η	k				
		0	1	5	10	50
0	1	3.30	8.9	14.95	16.77	18.00
0.05		3.10	8.354	14.05	15.767	16.76
0.10		2.91	7.825	13.158	14.772	15.71
0.15		2.72	7.301	12.28	13.79	14.67
0.20		2.53	6.78	11.41	13.01	13.64
0	5	1.58	4.27	7.16	8.19	8.73
0.05		1.51	3.97	6.66	7.49	7.97
0.10		1.35	3.54	5.94	6.67	7.11
0.15		1.196	3.12	5.24	5.89	6.27
0.20		1.05	2.72	4.55	5.13	5.46
0	10	1.51	4.05	6.78	7.6	8.12
0.05		1.43	3.66	6.12	6.87	7.33
0.10		1.25	3.26	5.43	6.102	6.5
0.15		1.10	2.88	4.78	5.37	5.72
0.20		0.95	2.51	4.16	4.67	4.98
0	50	1.48	3.97	6.69	7.53	8.03
0.05		1.33	3.55	5.99	6.74	7.18
0.10		1.18	3.14	5.31	5.97	6.37
0.15		1.03	2.75	4.65	5.24	5.58
0.20		0.89	2.38	4.02	4.53	4.83

5 Conclusion

In the present paper, buckling analysis of thick cylindrical shells with simply supported boundary conditions under the action of different types of mechanical loadings is car-

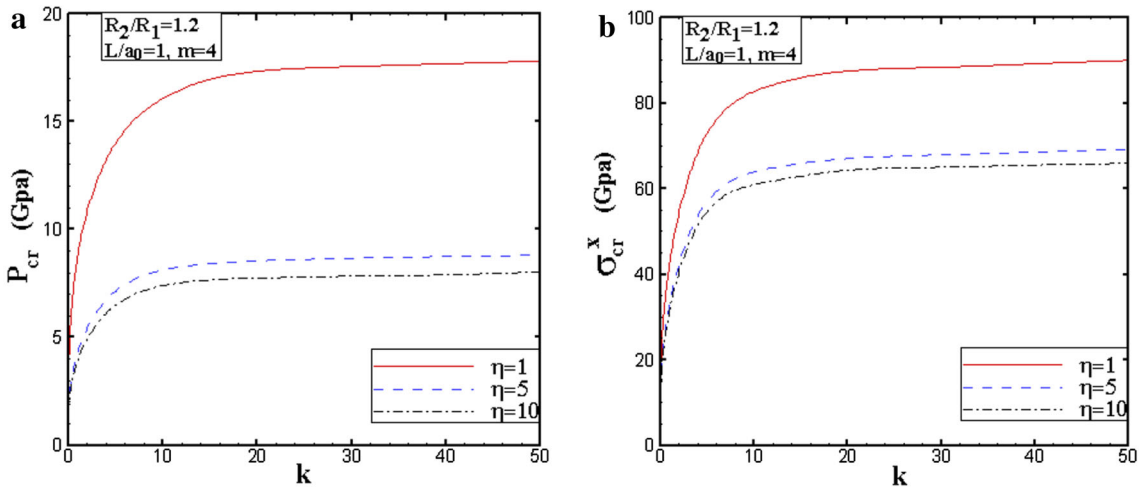

Fig. 10 Variation of critical load with k for FG thick shell, ($\alpha = 1$, $\beta = 0$). **a** External pressure. **b** Axial compression

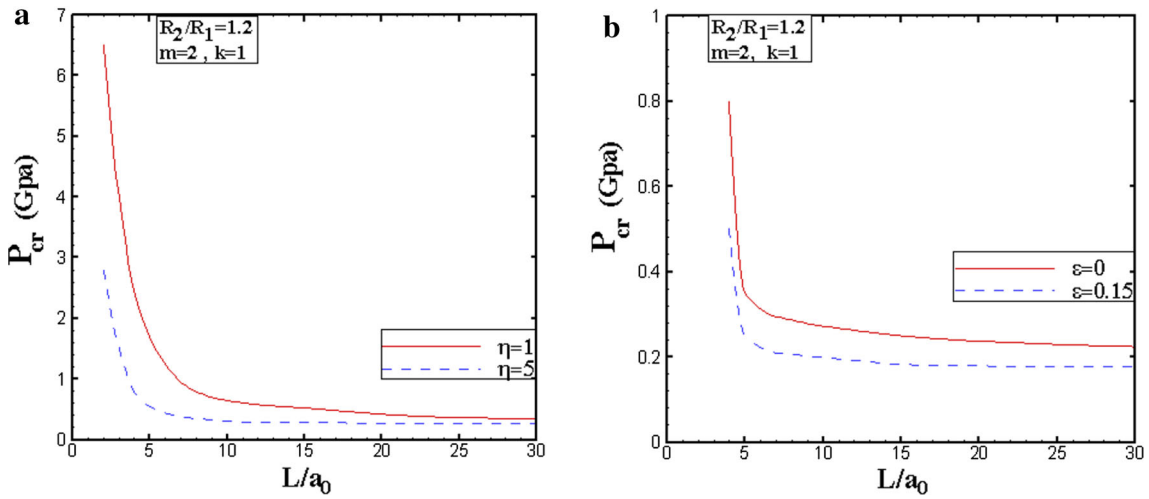

Fig. 11 Variation of buckling pressure of an FG shell with L/a_0. **a** Variable thickness. **b** With imperfection

ried out. Material properties are assumed to be temperature-independent and graded through the thickness according to a simple power law function in terms of the volume fractions of constituents. Differential equations are developed and then discretized and solved by differential quadrature method. The effects of thickness variation and imperfection on the critical buckling load of the shell are investigated. Numerical results for buckling loads of alumina–aluminum FG cylindrical shells are presented. Effects of the volume fraction of constituents, shell geometric parameters, thickness variation amplitude, imperfection parameter and loading conditions on the buckling behavior of FG cylindrical shells are investigated. From the present study, the following conclusions are obtained:

- The critical buckling pressure of an FG cylindrical shell under combined axial and lateral pressure loading decreases as the load factor increases.
- For FG thick cylindrical shells under mechanical loads, an increase in the volume fraction of ceramic constituent leads to an increase in the critical load.
- For a shell with variable thickness, buckling load decreases as the thickness variation amplitude factor η increases. It is observed that such reduction is higher in the case of uniform lateral pressure loading than the axial loading case.
- In the case of uniform lateral pressure loading, buckling load reduction is linear for small values of the thickness imperfection parameter, ε. It is also noted that buckling

load variation is more sensitive to the imperfection parameter ε in the case of pure lateral pressure than the axial loading case.

References

1. Koiter, W.T.: Buckling of cylindrical shells under axial compression and external pressure: thin shell theory new trends and applications. In: Olzak, W. (ed.) CISM Courses and Lectures, vol. 40, pp. 77– 87. Springer, New York (1980)
2. Elishakoff, I.; Li, Y.; Starners, J.H.: Non-Classical Problem in Theory of Elastic Stability. pp. 43–98. Cambridge University Press, Cambridge (2001)
3. Gusic, G.; Combescure, A.; Jullien, J.F.: The influence of circumferential thickness variations on the buckling of cylindrical shells under lateral pressure. Comput. Struct. **74**, 461–477 (2000)
4. Nguyen, T.H.L.; Thach, S.S.H.: Stability of cylindrical panel with variable thickness. Vietnam J. Mech. VAST. **28**(1), 56–65 (2006)
5. Nguyen, T.H.L.; Thach, S.S.H.: Influence of the thickness variation and initial geometric imperfection on the buckling of cylindrical panel. In: Proceeding of the 8th Vietnamese Conference on Mechanics of Solids, Thai Nguyen, pp. 491–499 (2006)
6. Nguyen, T.H.L.; Elishakoff, I.; Nguyen, T.V.: Buckling under external pressure of cylindrical shell with variable thickness. Int. J. Solids Struct. **46**, 4163–4168 (2009)
7. Elishakoff, I.; Li, Y.W.; Starnes, J.H.: The combined effect of the thickness variation and axisymmetric initial imperfection on the buckling of the isotropic cylindrical shell under axial compression. Preliminary Report, Florida Atlantic University (1992)
8. Koiter, W.T.: The effect of axisymmetric imperfection on the buckling of cylindrical shells under axial compression. Akademie van Wetenschappen-Amsterdam, Ser. B **66**, 265–279 (1963)
9. Akbari Alashti, R.; Ahmadi, S.A.: Buckling of imperfect thick cylindrical shells and curved panels with different boundary conditions under external pressure. J. Theor. Appl. Mech. **52**(1), 25–36 (2014)
10. Koiter, W.T.; Elishakoff, I.; Li, Y.W.; Starnes, J.H.: Buckling of axially compression imperfect cylindrical shells of variable thickness. In: Proceedings of the 35th (AIAA/ASME/ASCE/AHS/ASC) Structural Dynamics and Materials Conferences, Hilton Head, pp. 277–289 (1994)
11. Sofiyev, A.H.: The buckling of an orthotropic composite truncated conical shell with continuously varying thickness subject to a time dependent external pressure. J. Compos. Part B **34**, 27–233 (2003)
12. Civalek, O.: A parametric study of the free vibration analysis of rotating laminated cylindrical shells using the method of discrete singular convolution. J. Thin-Walled Struct. **45**, 692–998 (2007)
13. Mirfakhraei, P.; Redekop, D.: Buckling of circular cylindrical shells by the differential quadrature method. J. Press. Vessel. Pip. **75**, 347–353 (1998)
14. Civaleka, O.: Application of differential quadrature (DQ) and harmonic differential quadrature (HDQ) for buckling analysis of thin isotropic plates and elastic columns. J. Eng. Struct. **26**, 171–186 (2004)
15. Koizumi, M.: The concept of FGM. Ceramic Transactions. Funct. Gradient Mater. **34**, 3–10 (1993)
16. Lai, W.M.; Rubin, D.; Krempl, E.: Introduction to Continuum Mechanics, 3rd edn. Butterworth-Heinemann, Massachusetts (1996)
17. Ciarlet, P.G.: Mathematical Elasticity. Three Dimensional Elasticity, vol. I. North-Holland, Amsterdam (1988)
18. Shu, C.: Differential Quadrature and Its Application in Engineering. Springer, London (2000)
19. Kardomateas, G.A.: Benchmark three-dimensional elasticity solution for the buckling of thick orthotropic cylindrical shells. J. Appl. Mech. (ASME) **5**, 569 (1996)
20. Timoshenko, S.P.; Gere, J.M.: Theory of Elastic Stability. McGraw Hill, New York (1961)
21. Flugge, W.: Stresses in Shells. Springer, Berlin (1960)